WPo3.3

SIMULATION OF THE IONIZATION DYNAMICS OF ALUMINUM IRRADIATED BY INTENSE SHORT-PULSE LASERS

J. J. MacFarlane, I. E. Golovkin, and P. R. Woodruff
Prism Computational Sciences, Madison, WI 53711
Tel: (608) 280-9179; Fax: (608) 268-9180; E-mail: jjm@prism-cs.com

D. R. Welch and B. V. Oliver
Mission Research Corporation, Albuquerque, NM

T. A. Mehlhorn and R. B. Campbell
Sandia National Laboratories, Albuquerque, NM

ABSTRACT

We present results from time-dependent collisional-radiative simulations of the ionization dynamics of Al at near-solid density. Calculations were performed for a range of plasma and energetic electron parameters representative of those obtained from particle-in-cell simulations[1] of the heating of Al by an intense, short-pulse laser. We discuss the influence of energetic electrons on the ionization dynamics of the Al and its emission spectrum.

I. INTRODUCTION

Intense short-pulse lasers can be used to rapidly heat materials to produce hot plasmas at near-solid density. Ultrashort-pulse laser beams with intensities ~ 10^{16} – 10^{20} W/cm^2 and pulse widths ~ 10^{-1} ps can be used to study strongly coupled plasmas[2-4], to create sources for x-ray radiography, and to investigate fast ignitor concepts for inertial confinement fusion[5-7]. The very rapid deposition of laser energy near the surface of a material results in very steep plasma gradients and the production of energetic electrons that can propagate rapidly through the material. These energetic electrons are capable of influencing the ionization dynamics and spectral characteristics of the material.

In this paper, we present the results of collisional-radiative calculations for aluminum at near-solid density for a range of plasma conditions and energetic electron distributions relevant to short-pulse laser experiments. Particle-in-cell (PIC) calculations performed using the LSP hybrid fluid-kinetic, electromagnetic simulation code[1,8,9] predict that, for a 10 ps duration, 10^{18} W/cm^2 beam irradiating a 200 µm-thick Al foil, plasma temperatures ranging from tens of eV up to a few keV are achieved while the Al is near solid density. In addition, an energetic electron component is generated that may be capable of affecting the ionization dynamics and spectral properties of the material.

Following a description of our simulation models in Section II, we discuss results from simulations performed to examine: time-scales required to reach steady-state, the role of energetic electrons in affecting the ionization and spectral properties of the material.

II. MODELING

To calculate the properties of Al in the presence of energetic electrons, we use a time-dependent collisional-radiative model that includes the following processes: electron-impact ionization, recombination, excitation, and deexcitation for a general, non-Maxwellian electron distribution, $f(e)$, radiative recombination, spontaneous decay, dielectronic recombination, autoionization, electron capture, photoionization, photoexcitation, and simulated recombination and deexcitation. In treating the electron distribution, we use a two-component model:

$$f(\boldsymbol{e}) \;=\; (1 - \boldsymbol{g}_H)\;\; f_M(T_1)\; +\; \boldsymbol{g}_H\; f_H(\boldsymbol{e}) \qquad (1)$$

where $f_M(T_1)$ is a Maxwellian component with temperature T_1, $f_H(\boldsymbol{e})$ is a "hot" component which in general need not be a Maxwellian distribution, and $\boldsymbol{g}_H$ is the fraction of hot, non-Maxwellian electrons.

The electron-impact collisional excitation and ionization cross sections utilized in the collisional-radiative simulations were computed using a distorted wave model. Collisional rates are obtained by integrating the cross sections over the generalized electron energy distribution[10], $f(\boldsymbol{e})$. In the case of 3-body recombination, which involves the double integration over the electron distribution functions, we approximate the non-Maxwellian component in Eq. (1) by a Maxwellian with an effective temperature, T_H, as is done in Ref. 10, thereby avoiding the need for time-consuming double integration. Photoionization cross sections, oscillator strengths, autoionization rates, and energy levels are obtained from Hartree-Fock calculations. Calculation of the above raw atomic data was performed using the ATBASE package[11].

In these calculations, the atomic model used for aluminum consisted of ~ 200 levels from all ionization stages, and used configuration-averaged atomic modeling. For each ion, excited states up through $n = 4$ were included. For F-like through Li-like aluminum, autoionizing states with an open K-shell vacancy were included so that Kα transitions of the type $1s^1\,2s^m\,2p^n \to 1s^2\,2s^m\,2p^{n-1}$ were included in the calculation of emission spectra.

Continuum lowering effects are modeled using an occupation probability model[12], supplemented by the ionization potential depression formalism of More[13]. The occupation probability model produces a continuous reduction in the effective statistical weights of energy levels with increasing density, so that the relatively high-n states cannot be populated at high densities. This occupation probability formalism compares favorably with results from ion microfield calculations of argon at high densities[14] using the *APEX* code[15]. The ionization energy thresholds are depressed using the More model, which results in an enhancement of ionization rates and a shift in the location of bound-free edges in computed spectra.

The above models are part of the physics package contained in the *SPECT3D* imaging and spectral analysis suite,[16] a package that is used in post-processing output from radiation-hydrodynamics codes and PIC codes. In the calculations presented below, we use the *PrismSPECT* code, as it utilizes the same physics package, but more conveniently allows for the setup and analysis of problems involving single volume elements of uniform temperature and density.

III. RESULTS

In this section, we discuss results illustrating the ionization dynamics of solid-density Al and the effect of the hot electrons. Figure 1 shows the time-dependent mean charge state, $\overline{Z}$, for a hot electron fraction of 0% (circles), 1% (squares), and 10% (diamonds). The curves with filled symbols correspond to Al at a temperature of $T = 100$ eV, while those with open symbols correspond to Al at $T = 1$ keV. In all cases the temperature of the hot electron component is $T_H = 10$ keV. For the $T = 100$ eV case, a hot electron fraction of ~ 1% begins to change $\overline{Z}$ by a few tenths of a charge state. For a 10% hot electron fraction the change in $\overline{Z}$ is much more significant – about 2 full charge states. The effect of the hot electrons can be very pronounced for Al at $T \sim 100$ eV because in the absence of these relatively energetic electrons, there are few electrons with sufficient energy to promote electrons to relatively high ionization stages (such as Be-like and Li-like Al, which have ionization thresholds of ~ 330 - 400 eV).
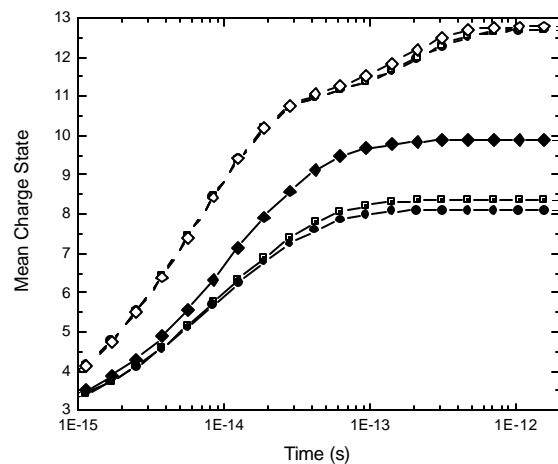

Figure 1. Calculated mean charge state vs. time for a solid density Al plasma at T = 100 eV (filled symbols) and T = 1 keV (open symbols). The temperature of the hot electrons is T_H = 10 keV, and the hot electron fraction is 0% (circles), 1% (squares), and 10% (diamonds).

2

For a $T = 1$ keV Al plasma, the hot electron component does not significantly change the ionization dynamics for Al because there are an abundance of electrons from the thermal (Maxwellian) component to ionize the Al well into the K-shell.
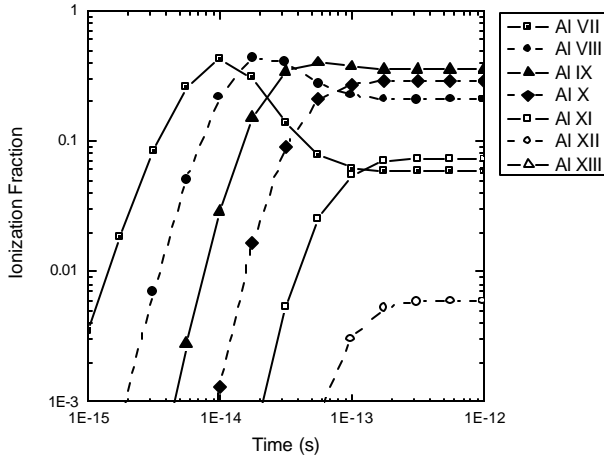

Figure 2. Calculated mean charge state vs. time for a solid density Al plasma at T = 100 eV and with no hot electrons.

Figures 2 and 3 show the time-dependent ionization fractions for N-like Al (Al VII) through H-like Al (Al XIII) for simulations with no hot electrons and with a 10% hot electron fraction, respectively. In these calculations, the solid-density Al was at $T = 100$ eV, and the hot electron temperature was $T_H = 10$ keV. Note that in the absence of the hot electron component (Fig. 2), the ionization fractions of He-like and H-like Al remain very small. The effect of the hot electron component is to significantly enhance the populations of higher ionization stages. Figure 3 shows that significant populations of He-like (24%) and H-like (5%) Al are achieved even though the electron temperature in the bulk of the solid-density Al is only 100 eV.

Plasmas containing energetic electrons are capable of populating highly-excited states with K-shell vacancies through inner-shell transitions of the type $1s^2 2s^m 2p^n \rightarrow 1s^1 2s^m 2p^{n+1}$. This can produce K$\alpha$ satellite line emission in the $\sim 1485 - 1585$ eV spectral region from cold Al up through Li-like Al. Such satellite emission has been observed in a variety of laser experiments (see Ref. 4 and references therein).
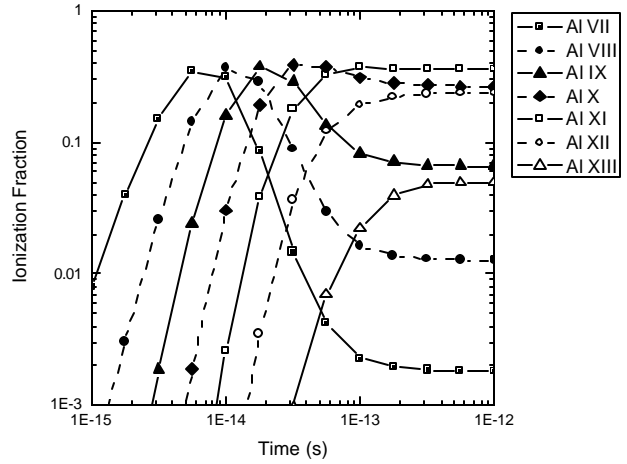

Figure 3. Same as Figure 3, but with a 10% hot electron component with $T_H = 10$ keV.

Figure 4 shows the evolution of the calculated emission spectrum from a $T = 100$ eV Al plasma with a 10% hot electron fraction (which corresponds to the ionization fractions in Figure 3). Note that emission at early times is dominated by transitions from lower ionization stages (at h? = 1485 – 1500 eV). As the aluminum ionizes through the L-shell, emission from Kα satellites is seen at slighter higher photon energies. (Each emission feature between the "cold" Kα line at 1485 eV and the He$_a$ line at 1598 eV corresponds to emission from a different ionization stage.)
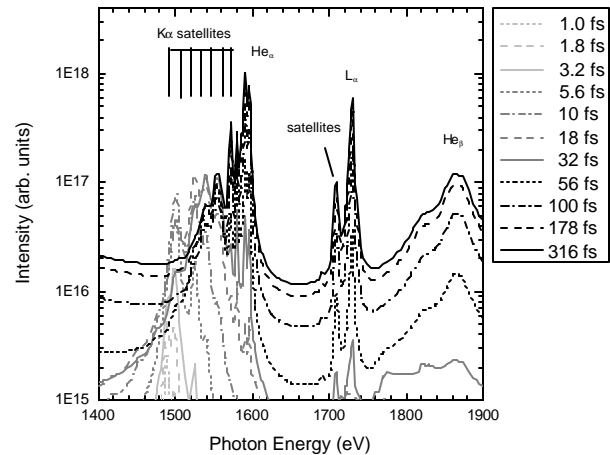

Figure 4. Calculated spectra at simulation times ranging from 1 fs to 316 fs for a solid density Al plasma at T = 100 eV with a 10% hot electron component with $T_H = 10$ keV.

After about 50 – 100 fs, emission from He-like and H-like Al becomes prominent. By 300 fs, the atomic level populations have attained their steady-state values, and the spectrum changes little after this time. We note that the relatively broad emission features from the Ka satellites and the He-like and H-like resonance lines in Figure 4 are qualitatively consistent with spectra observed from short-pulse laser experiments at near-solid density.[4]

IV. CONCLUSIONS

Time-dependent collisional-radiative simulations have been performed for solid-density aluminum to examine the effect of energetic electrons on the ionization dynamics and spectral characteristics of the Al. Our simulations indicate that a hot electron component of $\gtrsim$ a few percent can significantly alter the ionization distribution for solid-density Al at $T \sim 10^2$ eV. Simulated spectra show the evolution of inner-shell Ka satellite emission lines and He-like and H-like resonance lines that are qualitatively consistent with spectral measurements obtained in previous experiments.

V. ACKNOWLEDGEMENTS

REFERENCES

1   D. R. WELCH, B.V. OLIVER, J. J. MACFARLANE, R. B. CAMPBELL, and T. A. MEHLHORN, *Proceedings of the 3rd International Conference on Inertial Fusion Science and Applications* (2003).

2   K. EIDMANN, U. ANDIEL, E. FORSTER, *et al., Proceedings of the 12th Topical Conference on Atomic Processes in Plasmas,* p. 238 (2000).

3   K. EIDMANN, J. MEYER-TER-VEHN, T. SCHLEGEL, *et al., Phys. Rev. E* **62**, 1202 (2000).

4   A. SAEMAN, K. EIDMANN, I. E. GOLOVKIN, *et al., Phys. Rev. Lett.* **82**, 4843 (1999).

5   M. TABAK, J. HAMMER, M. E. GLINSKY, *et al., Physics of Plasmas* **1**, 1626 (1994).

6   M. H. KEY, M. D. CABLE, T. E. COWAN, *et al., Physics of Plasmas* **5**, 1966 (1998).

7   K. YASUIKA, M. H. M. KEY, S. P. HATCHETT, *et al., Rev. Sci. Instrum.* **72**, 1236 (2001).

8   D. R. WELCH, D. V. ROSE, D. V. OLIVER, *et al., Nucl. Instrum. & Methods Phys.Res. A* **464**, 134 (2001).

9   T. P. HUGHES, S. S. YU, and R. E. CLARK, *Physics Review ST-AB* **2**, 110401 (1991).

10   F. B. ROSMEJ, D. H. H. HOFFMANN, W. SUSS, *et al., Phys. Rev. A* **63**, 032716 (2001).

11   P. WANG, J. J. MACFARLANE, T. A. MEHLHORN, *et al., Phys. Rev. E* **48**, 3934 (1993); P. WANG, *ATBASE Users Guide*, Univ. Wisconsin Report UWFDM-942 (1993).

12   D. G. HUMMER, D. MIHALAS, *Astrophys. J.* 331, 794 (1988).

13   R. M. MORE, in *Applied Atomic Collision Physics*, **2**, Academic Press, New York (1982).

14   D. A. HAYNES, *private communication* (2001).

15   C. A. IGLASIUS, *et al., Phys. Rev. A* **31**, 1698 (1985).

16   J. J. MACFARLANE, I. E. GOLOVKIN, P. R. WOODRUFF, *et al.,* Prism Computational Sciences Report *PCS-R-045* (2003).